metals

MDPI

Article

Role of Microstructure Heterogeneity on Fatigue Crack Propagation of Low-Alloyed PM Steels in the As-Sintered Condition

Saba Mousavinasab and Carl Blais *

Département de génie des mines, de la métallurgieet des matériaux, Université Laval, Québec, QC G1V 0A6, Canada; saba.mousavinasab.1@ulaval.ca

* Correspondence: carl.blais@gmn.ulaval.ca; Tel.: +1-418-656-2049

Academic Editor: Filippo Berto

Received: 17 November 2016; Accepted: 14 February 2017; Published: 17 February 2017

Abstract: Due to their lower production costs, powder metallurgy (PM) steels are increasingly being considered for replacing wrought counterparts. Nevertheless, the presence of a non-negligible volume fraction of porosity in typical PM steels makes their use difficult, especially in applications where cyclic loading is involved. On the other hand, PM offers the possibility of obtaining steel microstructures that cannot be found in wrought. Indeed, by adequately using alloying strategies based on admixing, pre-alloying, diffusion bonding or combinations of those, it is possible to tailor the final microstructure to obtain a distribution of phases that could possibly increase the fatigue resistance of PM steel components. Therefore, a detailed study of the effect of different microstructural phases on fatigue crack propagation in PM steels was performed using admixed nickel PM steels (FN0208) as well as pre-alloyed PM steels (FL5208). Specimens were pressed and sintered to a density of 7.3 g/cm^3 in order to specifically investigate the effect of matrix microstructure on fatigue properties. Fatigue crack growth rates were measured at four different *R*-ratios, 0.1, 0.3, 0.5 and 0.7 for both PM steels. The negative effect of increasing the *R*-ratio on fatigue properties was observed for both alloys. The crack propagation path was characterized using quantitative image analysis of fracture surfaces. Measurements of roughness profile and volume fractions of each phase along the crack path were made to determine the preferred crack path. Weak Ni-rich ferritic rings in the FN0208 series (heterogeneous microstructure) caused a larger crack deflection compared to the more homogeneous microstructure of the FL5208 series. It was determined that, contrary to results reported in literature, crack propagation does not pass through retained austenite areas even though fatigue cracks propagated predominantly along prior particle boundaries, i.e., intergranular fracture.

Keywords: PM steels; heterogeneous microstructure; retained austenite; fatigue crack growth; crack path tortuosity

1. Introduction

Utilization of powder metallurgy (PM) steel components has significantly increased in recent years due their ability to be processed to near-net shapes, their intrinsic sustainability as well as their lower production costs. Most of the applications targeted by powder metallurgy are found in the automotive industry. Moreover, these applications increasingly involve undergoing cyclic loading that require better or equivalent fatigue properties compared to their wrought counterparts [1,2]. Fatigue is a complex phenomenon in PM steels since it is controlled by several characteristics. Porosity and matrix microstructure are the two most important parameters that need to be considered when studying the mechanical properties of PM parts [3].

Porosity reduces the effective load bearing cross section, through which mechanical properties such as strength and ductility are negatively affected [4–6]. Pores can also change the stress distribution at micro-levels, leading to stress concentration at the pores. Hence, the volume fraction of porosity is an important parameter that affects mechanical properties, especially fatigue resistance [7]. In low density parts, total volume of porosity is the major parameter on mechanical properties, whereas in high density ones, pore characteristics including size, shape and distribution as well as matrix microstructure happen to be the dominant parameters [8].

Apart from porosity, the other specific feature of PM materials is their heterogeneous microstructure. Microstructure of a PM material depends on the production process and the alloying technique. Excluding the pre-alloying technique, the other ones namely admixed, diffusion alloyed and hybrid will typically result in a heterogeneous microstructure [9]. This heterogeneity occurs mainly because of the incomplete diffusion of alloying elements that occurs due to low diffusion rates of alloying elements, large particle size, high repulsion between elements due to their chemical potential and some processing variables such as insufficient sintering temperature and time [9,10]. For a given density, fatigue properties of a PM part are mainly controlled by its microstructure. The effect of microstructure gets more attraction when involving a PM steel with heterogeneous microstructure.

Fatigue crack propagation is controlled by local properties at the crack tip, through which the fatigue behavior of a material is determined. A fatigue crack will face different microstructural phases while propagating in a heterogeneous microstructure PM steel. Due to the interaction of a crack with other cracks and microstructural barriers, such as porosity and grain boundaries, crack growth rate can decrease or cracks can even be arrested and stopped [11]. The behavior of fatigue cracks confronting these phases has not been characterized with exactitude, thus leading to divergent points of view in the literature.

In a study by Andersson and Lindqvist [12], fatigue behavior of a heterogeneous PM steel (Fe-4Ni-1.5Cu-0.5Mo-0.8C) was studied through which austenite was characterized as a ductile phase that can delay or stop the crack propagation. In another study on a diffusion alloyed PM steel as base powder with a microstructure of ferrite, pearlite, martensite in Cu/Mo rich areas (sinter necks) and austenite in Ni-rich areas (around the pores), it was also observed that short cracks are stopped by austenitic areas, whereas the long ones circumvented them. Therefore, it would appear that both mechanisms lower the propagation rate of fatigue cracks in PM steel [3]. Bergmark and Alzati [13], investigated the short cracks in Fe-4Ni-2Cu-1.5Mo-0.7C PM steel, using successive grinding to obtain 3D crack path observations. They found that Ni-rich austenite could not retard crack propagation by itself and the reason for not seeing this propagation might be related to plastic deformation and smearing.

Although there exist several studies on the effect of microstructure on fatigue crack propagation in PM steels, unified conclusions have not yet been reached. Different approaches used for demonstrating the effect of microstructure on fatigue crack growth as well as unsupported interpretations based on insufficient results could be the reason for these contradictory deductions. In this study, in order to have a complete comprehension of the effect of different phases on fatigue crack propagation behavior of PM steels, fatigue crack growth rate of two common alloys with the same density but different microstructures (homogeneous and heterogeneous) were measured at four *R*-ratios. The crack path was thoroughly analyzed in optical microscopy to characterize the crack behavior in facing different microstructural phases. The two-parameter approach and crack closure were also considered to complete the investigation.

2. Materials and Experimental Procedure

2.1. Materials

Two common PM steels produced by different alloying strategies were chosen in order to provide two types of microstructures (heterogeneous and homogeneous). The powder mixture utilized for

obtaining the heterogeneous microstructure contained nickel (Vale Canada type 123) that was admixed to an iron powder (Rio Tinto Metal Powders Atomet 1001), whereas the powder mixture that yielded the homogeneous microstructure had chromium and molybdenum as alloying elements and was obtained using the pre-alloying technique (North American Höganäs Astaloy CrL). These alloys were selected based on their inclusions in MPIF standard 35 and by the fact that they have a similar content in alloying elements. Graphite additions (Asbury natural graphite grade 1651) were adjusted to yield a combined carbon content of 0.6 wt. % for both mixtures. The exact chemical compositions of the materials studied are given in Table 1.

The specimens were made using a double-press/double-sinter approach. The powder mixtures were pressed and sintered to achieve the same density of 7.3 g/cm^3. Final sintering was done at 1120 °C for 30 min in a 90%N_2-10%H_2 atmosphere. Archimedes' principle (MPIF standard 42) was used to measure the density of the samples. Porosity of the samples was also characterized in terms of size and shape distribution by image analysis.

Table 1. Main alloying elements of the studied materials (wt. %).

Alloy	Fe	C	Ni	Mo	Cr
Admixed (FN-0208)	bal.	0.6	2	-	-
Pre-alloyed (FL-5208)	bal.	0.6	-	0.2	1.4

2.2. Fatigue Crack Growth Tests

The specimens preparation as well as the fatigue crack growth testing were perfomed in accordance with ASTM-E647-13 standard [14]. The sintered samples were machined into standard compact C(T) specimens using electrodischarge machining (EDM). Fatigue crack growth experiments were conducted at room temperature on an MTS servo-hydraulic testing machine (model 810 with a load cell of 10 KN) operating at a sinusoidal frequency of 10 Hz. Humidity was recorded at all times and tests were conducted in relative humidity ranging between 25% and 38%.

In order to provide a sharpened fatigue crack and also to remove the effect of the machining at the notch, fatigue pre-cracking was perfomerd with an a/w ratio of 0.2 using a constant ΔK procedure. The fatigue crack growth rates experiments were conducted at constant R-ratio following a constant-force-amplitude test procedure. This test procedure is suitable for crack growth rates above 10^{-8} m/cycle (Paris regime), which is the area of interest in this research. In order to study the effect of microstructure at different fatigue conditions, four different R-ratios (0.1, 0.3, 0.5 and 0.7) were also considered. Crack lengths were recorded at recommended intervals using the compliance method.

2.3. Characterization Techniques

Investigations were performed on the fatigue fracture surfaces as well as sections taken from the fractured specimens. The fractured specimens were cut vertically, i.e., along the crack path in order to follow and study the crack propagation path. An electroless Ni-plating process was used to coat the fracture surfaces before the cut was made. This was done to protect the details of the crack path. The transverse cross-sections were then prepared using the standard procedure of metallographic sample preparation for PM specimens.

Digital image analysis techniques were used on the as-polished and the etched specimens to characterize pore morphology and measure the volume fraction of each phase respectively. The etched transverse cross-sections were also used to follow the crack path in optical microscopy. In order to perform the quantitative analysis of the fracture surface, the volume fraction of each phase as well as the crack length along the crack path in the Paris regime were measured using an image analysis software (Clemex Vision, Clemex Technologies Inc., Longueuil, QC, Canada). Microhardness tests were performed using a test force of 25 gf applied for 13 s to help ascertain phase determination. Fatigue fracture surfaces were also characterized using scanning electron microscopy (SEM, JEOL Ltd., Tokyo, Japan).

3. Results

3.1. Microstructure

The typical microstructure of admixed and pre-alloyed PM steels considered in this study is shown in Figure 1. It can be seen that the admixed nickel-containing PM steel shows a heterogeneous microstructure of pearlite (P), Ni-rich ferrite (F) and retained austenite (RA) while the pre-alloyed one has a homogeneous pearlitic microstructure. The volume fractions of microstructural phases and the microhardness values of each phase is shown in Table 2.

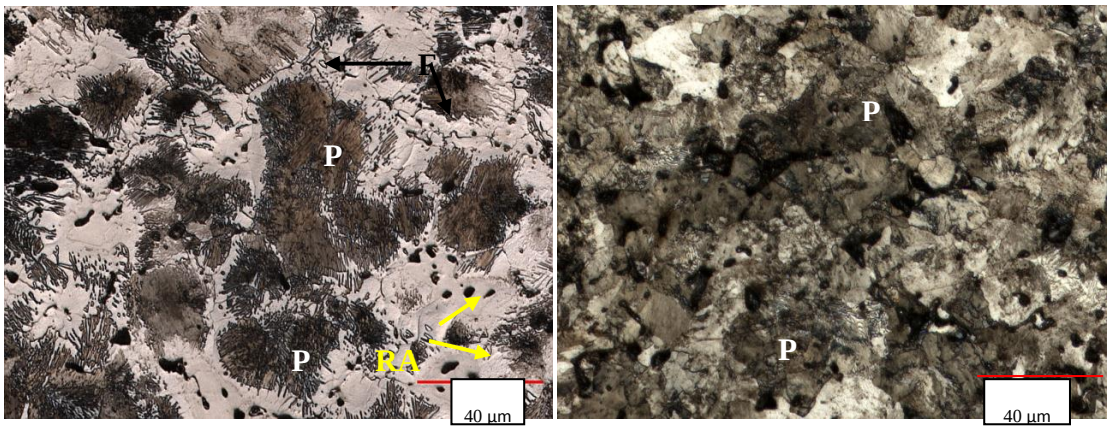

(**a**) (**b**)

Figure 1. Microstructure of (**a**) admixed and (**b**) pre-alloyed powder metallurgy (PM) steels, etched by Nital 2%.

Table 2. Volume fraction and micro-hardness values of the phases present in the two series of specimens studied.

Alloy / Hardness / Phase	Pearlite	Retained Austenite	Ni-Rich Ferrite
FN0208	69.5	9.7	20.8
Microhardness (HV)	280 ± 6	177 ± 10	193 ± 13
FL5208	98.5	1.5	0
Microhardness (HV)	290 ± 12	-	-

Low diffusion rate of nickel into an iron matrix at conventional sintering time and temperature as well as the repulsion between nickel and carbon atoms are responsible for the non-uniform distribution of nickel when this element is admixed. The Ni distribution gradient throughout the matrix leads to the formation of different microstructural phases upon cooling and consequently a heterogeneous microstructure is generated [15,16]. Ni-rich ferritic areas around pearlitic grains, bright areas in Figure 1, form due to the lack of carbon (Ni-rich/C-lean) for pearlite formation. Retained austenite regions are mainly present where prior Ni particles were located and nickel concentration is relatively high (more than 10 wt. %) [17].

Along with the microstructure, pore morphology (pore size and shape distribution) can also affect the fatigue crack propagation in high density PM steels [8]. Pore morphology was characterized on as-polished samples of both types of PM steels using optical microscopy. The filled area of each pore was measured and used as a criterion for its size. Pore shape factor was also calculated using the $F = 4\pi A/P^2$ expression, where A and P are the area and the perimeter of pores respectively. Figure 2 shows the size and shape distribution of the admixed and pre-alloyed PM steels. It can be seen that the difference between the pore morphology of the two alloys is negligible. Therefore, it can be concluded that any difference in their fatigue crack propagation behavior could be attributed to their

microstructures. In other words, the effect of microstructure can be studied and compared between the two alloys without the interference of the pore morphology effect.

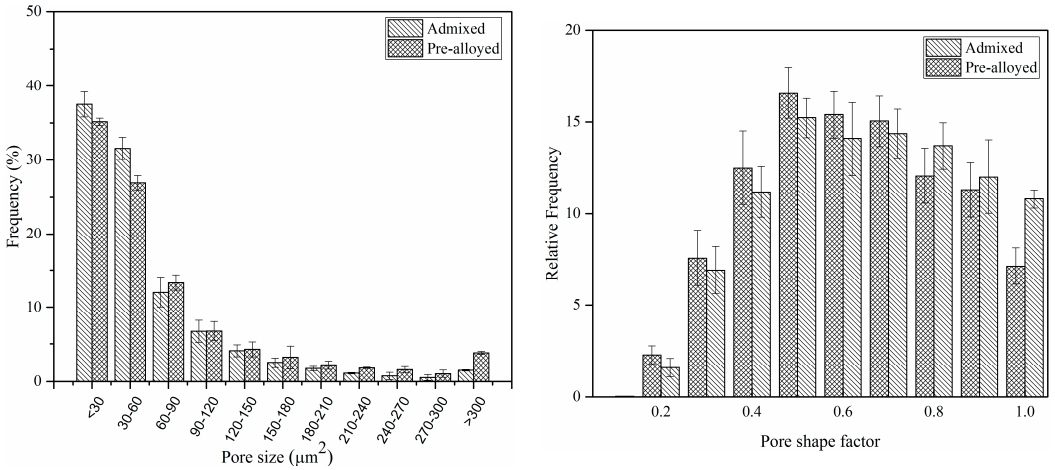

Figure 2. Distribution of the pore (**a**) size and (**b**) shape for both admixed and pre-alloyed sinter-hardened PM steels.

3.2. Fatigue Crack Growth Rate

Fatigue crack growth rate data acquired from the tests at four *R*-ratios are plotted against the stress intensity factor range on a logarithmic scale (Figure 3). Paris law ($da/dN = C\Delta k^m$) was then employed to the steady-state region of the plots to obtain m and C, the so-called Paris components, which are the empirical constants depending on material properties and testing conditions [18,19].

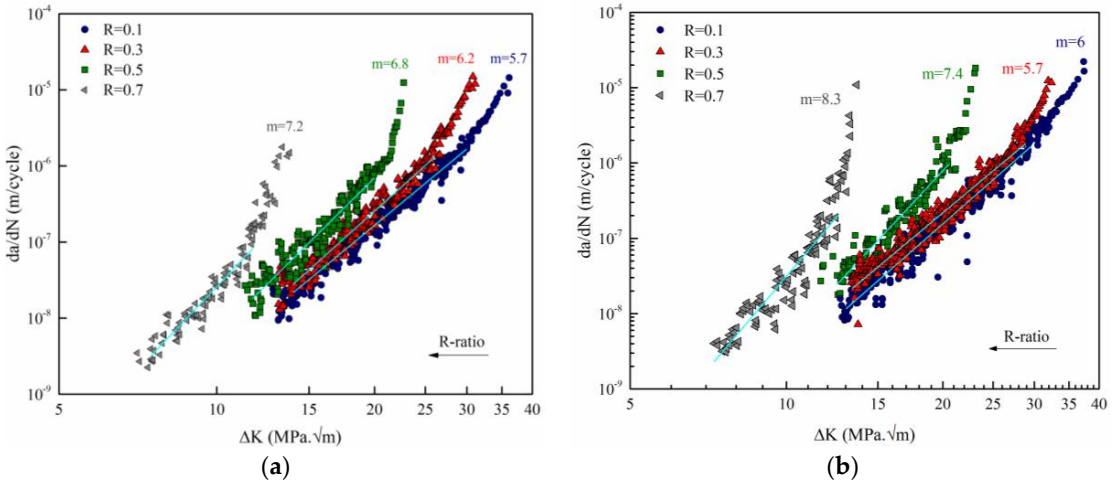

Figure 3. Fatigue crack growth rate vs. stress intensity factor range of the (**a**) admixed and (**b**) pre-alloyed PM steels at four tested *R*-ratios.

The variation of *m*—i.e., the slope of the linear section of the plot—versus *R*-ratio for both alloys is shown in Figure 4. According to Figures 3 and 4, it can be seen that the fatigue crack growth rate increases in both alloys by increasing the *R*-ratio due to the increase in minimum load. Nevertheless, this increase is more pronounced in the pre-alloyed PM steel, which is characterized by a homogeneous microstructure. In other words, the slope of the Paris regime, *m*, increases more rapidly by increasing the *R*-ratio. In pre-alloyed PM steels, *m* is almost the same for *R*-ratios of 0.1

and 0.3 but it increases intensively as the *R*-ratio increases from 0.3 to 0.7. This trend shows that the homogeneous microstructure is more sensitive to monotonic contribution since increasing the *R*-ratio indicates the higher dominant static effect [20].

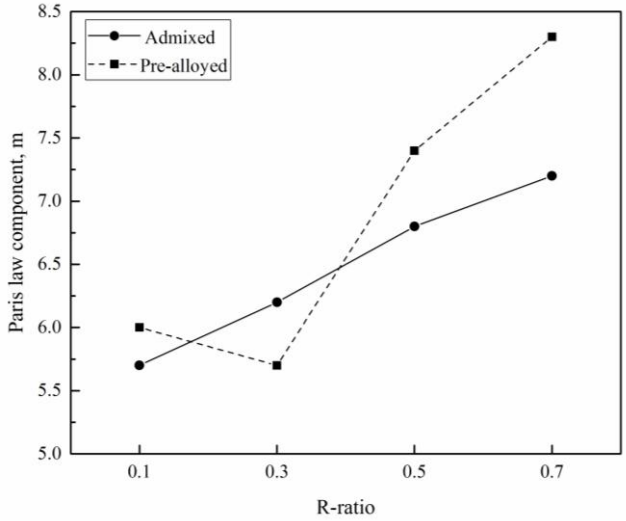

Figure 4. Variation of the slope (*m*) of the Paris regime versus the *R*-ratio.

4. Discussion

4.1. Fatigue Crack Growth (FCG) Behavior

The FCGs of the admixed and pre-alloyed PM steels should be compared quantitatively in order to understand the effect of microstructure homogeneity/heterogeneity on fatigue crack propagation. The FCGs for both types of microstructure were calculated using the Paris law and the derived Paris components, *m* and *C*. It is to be noted that *m* and *C* were derived from the fatigue crack growth rate (d*a*/d*N*) versus Δ*K* plots. The ratios of the calculated FCGs of the admixed PM steel to the FCG of the pre-alloyed PM steels were then obtained (for the purpose of comparison) and plotted against the stress intensity range (Δ*K*) at different *R*-ratios. Figure 5 shows the variation of the calculated ratios (d*a*/d*N* of the admixed to d*a*/d*N* of the pre-alloyed PM steels) against Δ*K* at four tested *R*-ratios.

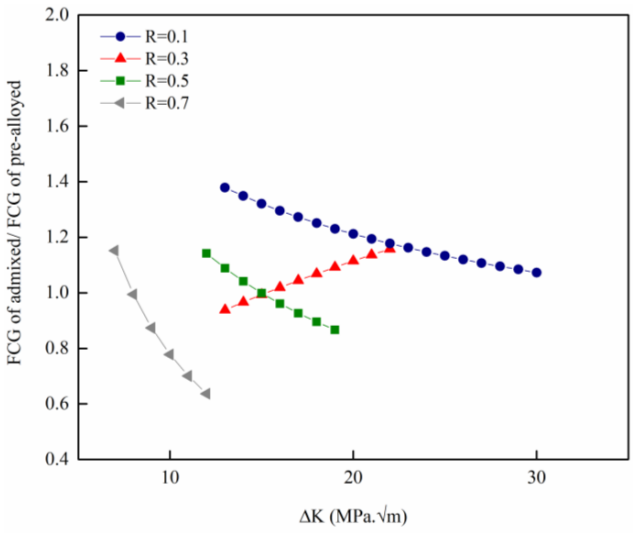

Figure 5. Variation of the fatigue crack growths' (FCGs') ratios (admixed/pre-alloyed) against Δ*K* in the Paris regime.

At R = 0.1, the FCG of the admixed PM steel is larger than the FCG of the pre-alloyed PM steel at low ΔKs (small crack lengths) but they became the same by increasing the ΔK. The calculated FCGs' ratio at R = 0.3 and 0.5 changes roughly between 0.8–1.2, throughout the applicable range of ΔK, which shows that the fatigue crack growth rates are almost the same for heterogeneous and homogeneous microstructures at these R-ratios. At R = 0.7, the fatigue crack growth rate in both types of alloys are similar at low ΔKs (small crack lengths) but it seems that by increasing the stress intensity factor range, the fatigue crack grew faster in the homogeneous microstructure since the calculated FCGs' ratio approaches the value of 0.6. The discussed trend of variation of fatigue crack growth rates with increasing R-ratio in both types of microstructures shows the higher sensitivity of the homogeneous microstructure to the localization of strain and plasticity at the crack tip.

In order to better understand the fatigue mechanisms involved in the tested PM steels, the two-parameter approach was also used. In this approach two parameters of K_{max} and ΔK are considered as the contributing parameters in fatigue crack growth. Therefore, there exists two crack tip driving forces and consequently two thresholds to be satisfied for crack growth to occur. ΔK vs. K_{max} plots that considered as fatigue maps are L-shaped plots that demonstrate the interplay of these two crack tip driving forces at any given crack growth rates [21]. These types of plots for both tested PM steels are shown in Figure 6. Since there were no experiments at negative R-ratios, the vertical parts of the plots are missing and the discussion will be made only using the horizontal part.

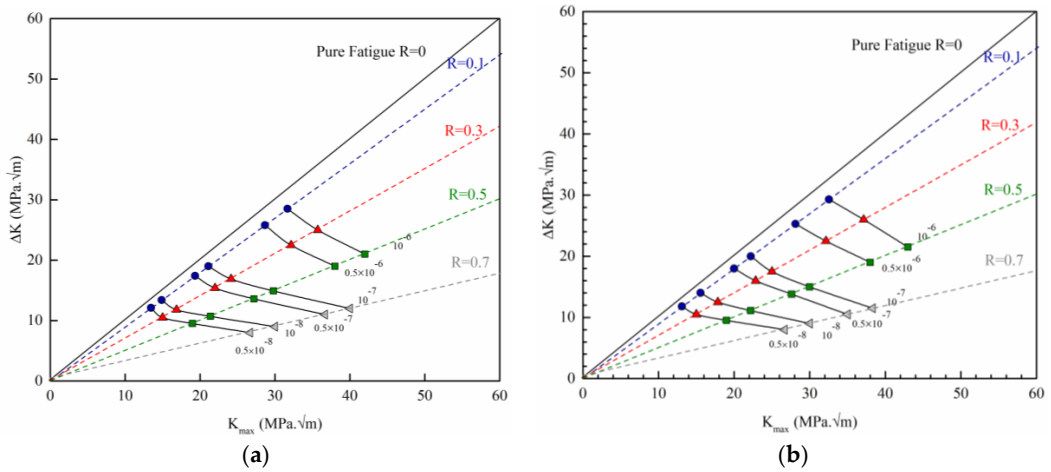

Figure 6. ΔK–K_{max} plots of (**a**) admixed (**b**) pre-alloyed PM steels, defining two limiting values at different crack growth rates.

By increasing the crack growth rate, the deviation (tilt) of the horizontal asymptote of the L-shape plots towards the K_{max} axis is slightly larger in the pre-alloyed PM steel compared to the one for the admixed PM steel. This shows that the pre-alloyed PM steel with a homogeneous microstructure is more affected by the K_{max}. In other words, this kind of microstructure is slightly more sensitive to monotonic contribution in fatigue damage. It can also be said that the crack tip is more sensitive to plasticity and strain localization in these kinds of microstructures [20–22].

Since there is a deviation (tilt) in horizontal asymptote of the L-shaped plots of both PM steels compared to a perfect L-shaped plot, it can be concluded that monotonic and/or environmental contribution were present for both types of microstructures [22]. In order to quantify this contribution, the crack growth trajectory maps can be used. By following the limiting values of the two driving forces (ΔK^* and K_{max}^*) at different crack growth rates in ΔK–K_{max} plots, the crack growth trajectory maps can be generated. A 45° line in these plots ($\Delta K^* = K_{max}^*$) is a pure fatigue line where only the cyclic damage is contributing in fatigue and any deviation from this line would determine the intrinsic mechanisms contributing in fatigue [21,22]. Figure 7 presents the trajectory maps of both types of alloys that have been derived from their ΔK–K_{max} plots.

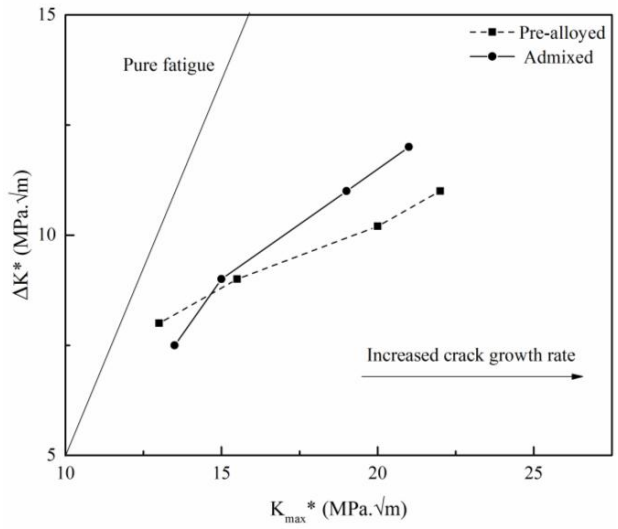

Figure 7. Crack growth trajectory maps of the admixed and pre-alloyed PM steels.

It can be seen that the trajectory path of the admixed PM steel is almost parallel to the pure fatigue line at low crack growth rates but deviates from it by increasing the crack growth rate. Being parallel to pure fatigue line at low crack growth rates indicates that fatigue is controlled only by cyclic plasticity whereas the divergence from this reference line at higher crack growth rates shows the effect of environment and monotonic contribution. The trajectory path of the pre-alloyed PM steel continuously diverges from the pure fatigue line with almost a constant angle.

Therefore, it can be concluded that the mechanisms are different in both types of microstructures, especially at low crack growth rates. The divergence from the pure fatigue line indicates that the environmental contribution increases with increasing crack growth rate. Besides, the deviation of the trajectory path towards the K_{max} axis, which is higher for the pre-alloyed PM steel, corresponds to superimposed K_{max} governing processes [20,22]. In other words, the amount of monotonic contribution is higher for the pre-alloyed steel with a homogeneous microstructure, which is in agreement with results of the variation of the slope of Paris regime, m, against the R-ratio.

4.2. Crack Closure Analysis

Fatigue crack closure should also be considered in studying the fatigue behavior of a material. Crack closure happens when two crack faces are in premature contact upon the unloading portion of a cycle. Elber [23] found out that due to the presence of the plastic zone at the wake of a fatigue crack, the crack could become closed far before the tensile stress reaches zero. A monotonic plastic zone, which is formed during loading to the maximum load, will lead to the permanent elongation in the loading direction. During unloading, this plastically elongated area will be under compression and consequently cause the premature crack closure even before reaching the minimum load. This type of crack closure is called plasticity-induced crack closure and it is reduced by increasing the R-ratio, i.e., increasing the minimum load [24,25].

When the crack is closed, the stress intensity at the crack tip decreases. Therefore, in order to analyze the degree of the crack closure, fatigue crack growth rates data should be plotted against ΔK_{eff}, which is equal to K_{max}–K_{open}. Fatigue crack closure were measured according to the ASTM E-647-13 guidelines using the load-displacement data obtained from the crack opening gauge during the test. Figure 8 shows the da/dN versus ΔK and ΔK_{eff} for both admixed and pre-alloyed PM steels at different R-ratios.

It can be seen that the amount of crack closure in pre-alloyed PM steels (Figure 8b) is the same at all R-ratios, i.e., it does not decrease by increasing the minimum load as expected [24,26]. This could be related to several causes such as different microstructure of PM steels compared to wrought ones

and/or other crack closure controlling mechanisms such as the mismatch between upper and lower fracture surfaces and mixed mode sliding of the crack. The presence of porosity in the microstructure of PM steels most likely changes the expected trend of plasticity induced crack closure with increasing *R*-ratio. Nevertheless, according to previous studies [20,27], the decreasing trend of crack closure with *R*-ratio was observed in PM steels with either heterogeneous or homogeneous microstructure. Therefore, there should be another mechanism involved in the crack closure of these PM steels.

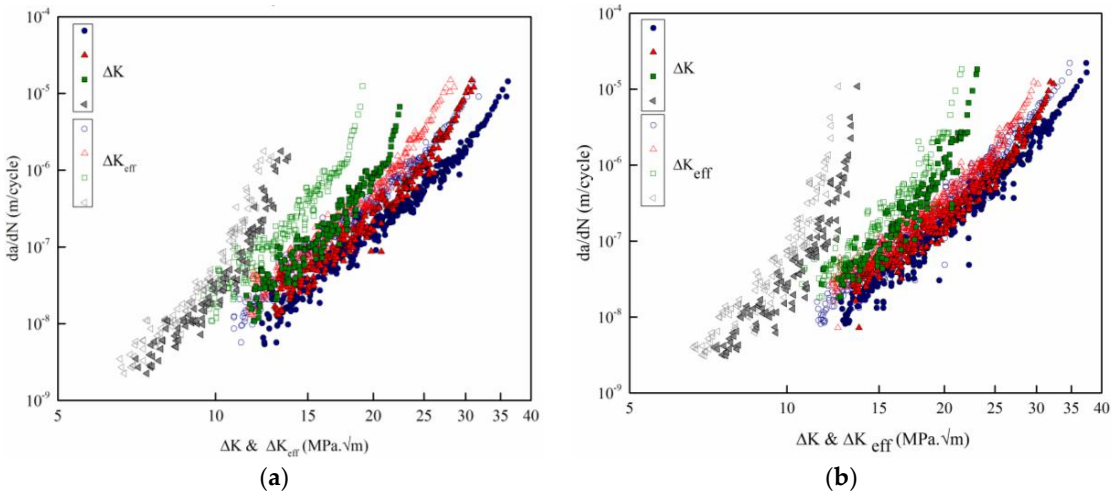

Figure 8. Fatigue crack growth rates of (**a**) admixed and (**b**) pre-alloyed PM steels versus ΔK and ΔK_{eff}.

Due to the fact that crack closure mechanisms could act synergistically, another mechanism or mechanisms are probably acting at the same time as the plasticity induced crack closure, causing the degree of the crack closure to be constant instead of decreasing (with increasing the *R*-ratio). The most probable mechanisms the mismatch between the upper and lower fracture surfaces that happens when two faces of the crack do not fit perfectly during unloading due to the crack deflection and/or the mixed mode sliding of the crack. This type of closure is called roughness-induced crack closure and is possible for both heterogeneous and homogeneous microstructures [24].

Figure 8a shows the degree of crack closure for the admixed PM steel at different *R*-ratios. It can be seen that the crack closure effect is almost constant for *R*-ratios of 0.1, 0.3 and 0.5, while it decreases when the *R*-ratio increases to 0.7. This diminution could be related to the formation of the reversed plastic zone that leads to the lower compression stress applied on the crack faces. The formation of this reversed plastic zone requires a sufficient increment in the local stress in the reversed direction and its size is around a quarter of the previous plastic zone [24]. The same as for the pre-alloyed PM steels, other closure mechanisms such as the mismatch between the upper and lower fracture surfaces and mixed mode sliding, might be contributing in the crack closure of the admixed PM steel that are causing the observed anomaly in the crack closure trend against the *R*-ratio. This phenomenon was observed in a recent article that studied similar PM steels [27].

4.3. Crack Path Analysis and Fractography

The effect of microstructure on fatigue crack growth behavior can be investigated using quantitative analysis of the fracture surface. This analysis can be done on a fracture surface as well as a fracture profile, which is the intersection of the fracture surface with a metallographic sectioning plane. A typical fracture profile is usually an irregular and complex line to which a profile roughness parameter (R_L) can be attributed. R_L is defined as follows:

$$R_L = \lambda_0 / L$$

where λ_0 is the actual measured length of fracture profile and L is equivalent straight path (projected length). R_L can vary between 1 and ∞ depending on the irregularity of the fracture profile [28,29]. This parameter can be used to quantify the crack deflection and could be an accurate criterion for comparing the fatigue crack paths in different microstructures. As mentioned above, metallographic sections along the crack paths (vertical sections) were made on each fracture surface. λ_0 was measured on micrographs obtained from the vertical sections and R_L was then calculated. Figure 9 shows the variation of profile roughness parameters for both alloys at different R-ratios.

It can be seen that fatigue crack has a tortuous path in both pre-alloyed and admixed PM steels with homogeneous and heterogeneous microstructures since R_L is larger than 1. Generally, a crack will change its path when confronting microstructural barriers or by passing through the grain and/or inter-particle boundaries. As previously observed by these authors [27] as well as being reported elsewhere in literature [20], a crack can be deflected by the Fe_3C lamellae of pearlite colonies. Since pearlite is the main constituent of the microstructure in both alloys (Table 1), it can be concluded that the reason for crack deviation in both types of microstructures is related to the presence of cementite lamellae. Moreover, R_L will be larger than one in the case of intergranular fracture in which the crack passes through boundaries, either grain boundaries or prior inter-particle boundaries for PM steels. Figure 10 shows the intergranular type of fracture at R = 0.1 and 0.7 for the admixed PM steel.

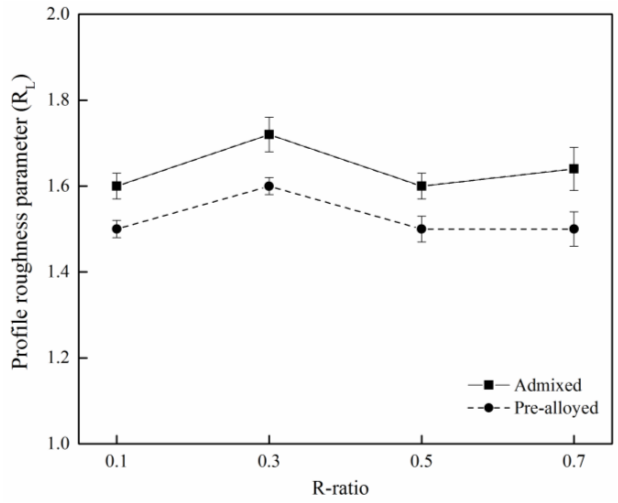

Figure 9. Profile roughness parameters for admixed and pre-alloyed at four R-ratios.

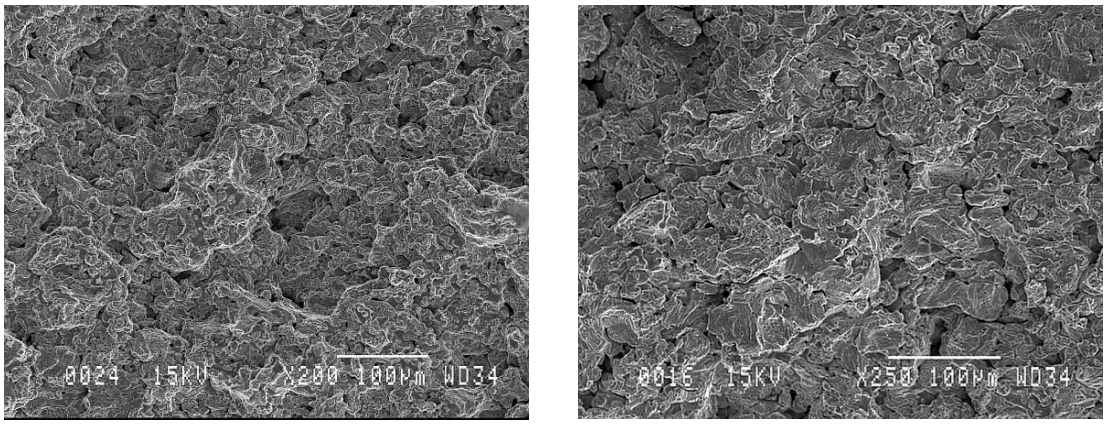

(**a**) (**b**)

Figure 10. Fracture surfaces of the admixed PM steels tested at (**a**) R = 0.1; (**b**) R = 0.7. Intergranular fracture is the principal mode of crack propagation in both micrographs.

Profile roughness parameters at four tested *R*-ratios for the pre-alloyed and admixed PM steels show that the amount of R_L has a small increase at $R = 0.3$, which could be related to the interaction of the crack with the pulled-out cementite lamellae from their pearlitic matrix during fatigue. This was previously observed by these authors for the same alloys but in the sinter-hardened condition as well as being reported in the literature [20,27]. After an increase in roughness parameter at the mentioned *R*-ratio, there is a decrease for both types of microstructures that could be attributed to the increase in the percentage of transgranular fracture brought about by increasing the minimum load, i.e., increasing the *R*-ratio. Fracture type (intergranular/transgranular) can be better studied using scanning electron microscopy. Figure 11 shows the SEM micrograph of the admixed PM steel at $R = 0.7$ at higher magnification. It can be seen that by increasing the minimum load, the fracture surface shows more transgranular fracture proving that the crack has the tendency of propagating through the grains rather than at grain/inter-particle boundaries at high *R*-ratios. It should be mentioned that the principal mode of fracture is still the intergranular one and only the percentage of the transgranular fracture has been increased by increasing the *R*-ratio.

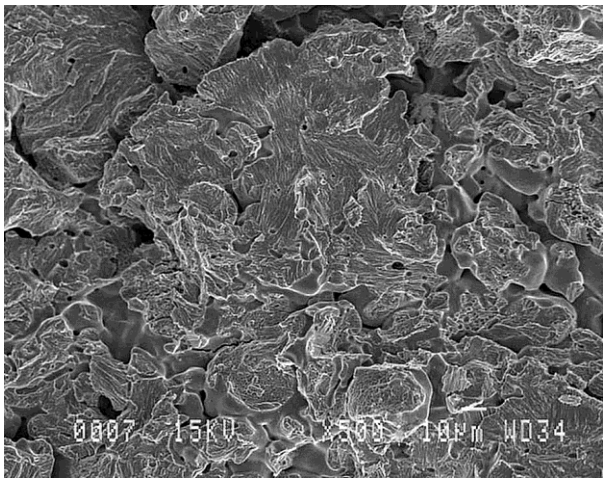

Figure 11. Fracture surface of the admixed PM steel at $R = 0.7$. The grains have been cut by the crack showing the transgranular fracture in some parts of the fracture surface.

The effect of microstructure heterogeneity/homogeneity can also be studied using the profile roughness parameter. As seen in Figure 9, there is a difference between the R_L of admixed and pre-alloyed PM steels at all *R*-ratios. The crack seems to be more deviated and tortuous in admixed PM steels with heterogeneous microstructure at all tested *R*-ratios although the difference is small. In order to investigate the reason for this difference, crack paths from the two types of microstructures were studied more precisely. Thus, the crack paths were followed in the area of interest (Paris regime) and volume fractions of the different phases found along the crack path were measured and compared to their amount in the bulk material. A ratio of the volume fraction of each phase in the crack path divided by its amount in bulk of the material was then calculated for all microstructural phases present to make the comparison easier. Figure 12 shows the calculated ratios for the admixed PM steels at four tested *R*-ratios. It should be noted that the mentioned ratio would be one in the case of the homogeneous microstructures since there was no difference between the volume fraction of microstructural phases along the crack path and in the bulk of the materials.

If there exists a difference between the volume fraction of a phase along the crack path compared to its amount in the material, the calculated ratio is then larger than one indicating that there is a preferred path for crack propagation in that specific phase [28]. As it can be seen in Figure 12, this ratio is three for Ni-rich ferrite in the admixed PM steels at all *R*-ratios. In other words, the amount of Ni-rich ferrite in the crack path is three times larger than its amount in the material indicating that this phase

is a preferred path for a fatigue crack to propagate. These Ni-rich ferritic regions are formed around pearlitic grains due to the non-homogeneous distribution of nickel and carbon throughout the iron matrix. Due to the rapid diffusion of carbon into the iron matrix and the repulsion between carbon and nickel during sintering at 1120 °C, particle peripheries and sinter necks will be Ni-rich/C-lean austenite, whereas the particle interiors (cores) will be C-rich/Ni-lean austenite. The C-rich/Ni-lean austenitic regions will transform into pearlite during cooling and will be surrounded by the transformed Ni-rich ferritic rings from Ni-rich/C-lean austenitic regions [16]. The presence of these weak ferritic rings around pearlite caused the difference between the degree of crack deviation in heterogeneous and homogeneous microstructures.

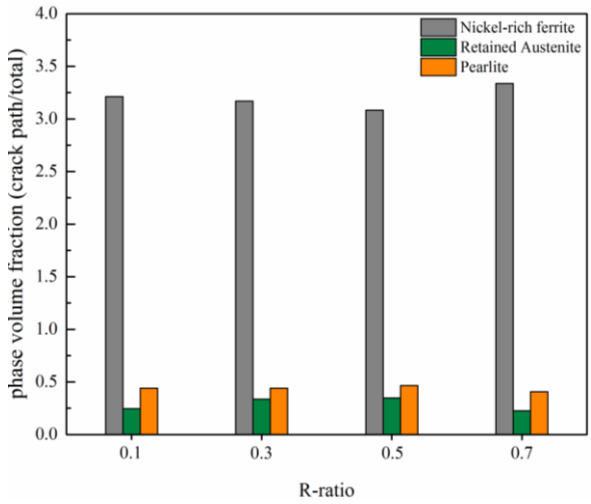

Figure 12. The ratios of the volume fraction of each phase in the crack path to its amounts in the material, for admixed PM steel at different *R*-ratios.

According to Figure 12, the crack has mostly passed through Ni-rich ferritic rings in the heterogeneous microstructure of admixed PM steels specimens. As stated above, Ni rich ferrite forms at the periphery of particles and/or sinter necks. Therefore, the results clearly indicate that the crack has propagated through prior particle boundaries in accordance with the intergranular nature of fracture characterized in SEM. Figure 13 shows a secondary crack in Ni-rich ferritic sinter necks in admixed PM steel. Retained austenite regions are formed mainly where the prior nickel particles were located. Therefore, these regions are also present at prior particle boundaries. Hence, it is expected that these regions were also being passed by the crack according to the intergranular nature of the fracture. On the other hand, the volume fraction of retained austenite along the crack path is less than half of its amount in the bulk material. This indicates that although these austenitic regions have relatively low strength, they are not preferred areas for fatigue crack propagation at least in comparison with Ni-rich ferritic regions. This can be related to the inherent ductility and toughness of retained austenite [8]. It should be mentioned that these conclusion were made based on the microstructure of one of the common admixed PM steels (FN0208) that usually have 10 vol. % of retained austenite and the results might be different when larger volume fractions of retained austenite are present.

These measures were only made on one half of the fractured surfaces, so it is important to understand and characterize the other half as well. In other words, to verify the above conclusions on fatigue cracks propagating preferably through specific microstructural phases, the other side of the crack path also needs to be investigated. On the other hand, aligning matching fracture surfaces is a daunting task especially when the latter where Ni-coated for metallography preparation. Thus, a strategy was devised using statistical techniques. Random micrographs were taken from each admixed PM steels' samples and the volume fractions of different prior particle boundaries were measured. Figure 14 shows a pie chart of the present prior particle boundaries in the admixed PM

steels series. This chart shows the probability of the presence of different phases on the other side of the crack. It can be seen that the highest percentage of the prior particle boundaries (65.36%) is between Ni-rich ferritic regions, and 30% of the boundaries correspond to retained austenite and ferrite. Therefore, it can be said that the previous conclusions about the preferred crack path through the Ni-rich ferritic regions is valid due to the high possibility of the presence of the same phase on the other side of the crack.

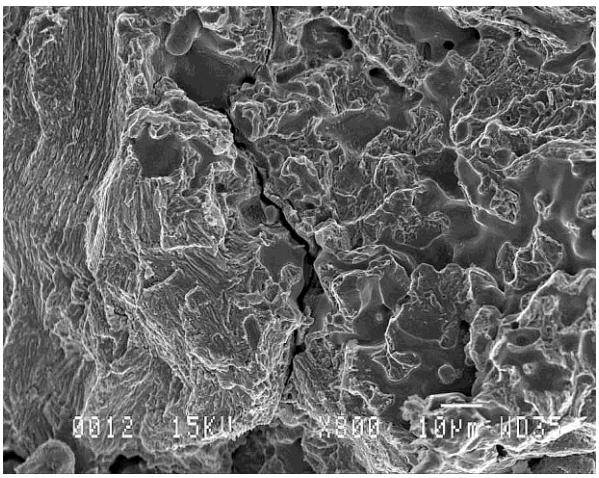

Figure 13. SEM micrograph of the fracture surface of the admixed PM steel at R = 0.5. A secondary crack has passed through a sinter neck.

Moreover, the amount of ferrite in the crack path will still be much larger than its amount in the bulk material even when considering the possibility of the presence of retained austenite in the other half. Figure 14 also shows that 4.5% out of 6% porosity of the admixed PM steels are located on ferritic boundaries. This amount should be subtracted from the calculated amount of ferrite along the crack path to obtain the exact volume fraction of this phase. This means that the crack has passed through pores as well as the microstructural phases but this was not distinguishable when measuring the volume fraction of each phase along the crack path.

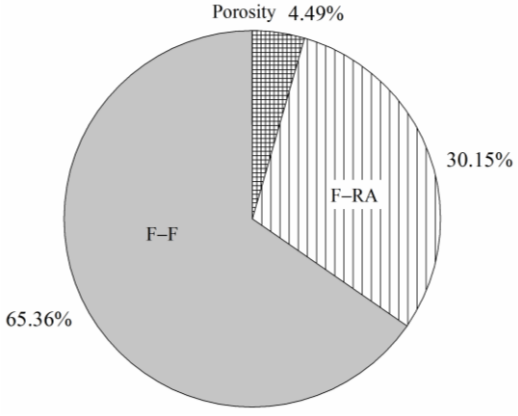

Figure 14. The pie chart of the present prior particle boundaries in admixed PM steels (F–F = Ferrite–Ferrite boundary; F–RA = Ferrite–Retained Austenite boundary).

According to Figures 5 and 9, it can be seen that at R = 0.3 and 0.5 fatigue crack growth rate is almost the same for both PM steels even though the crack path is more deviated in the admixed series with a heterogeneous microstructure. In the admixed PM steel with a heterogeneous microstructure made of pearlite, retained austenite and Ni-rich ferrite, the latter phase is responsible for crack

deviation, whereas in the homogeneous pearlitic microstructure of the pre-alloyed PM steel, it is the cementite lamellae that are causing the tortuous crack path. Having the same FCGs while having different degrees of crack tortuosity could be related either to the small difference in their degree of crack tortuosity and/or the fact that the crack deviation is not the only parameter affecting the fatigue crack propagation rate. It was previously reported that crack deflection increases the fatigue resistance of a material but its contribution is small [30].

The reason for having the same FCGs in two microstructures with different crack path tortuosity is most likely related to the higher fatigue crack propagation rate in low strength Ni-rich ferrite compared to high strength pearlite. In other words, a fatigue crack propagated faster in Ni-rich ferrite with a more tortuous path and consequently the combination of these two caused the same fatigue crack growth rates as the one with a less tortuous crack path in pearlite with higher strength. Hence, inherent properties such as the strength of the microstructural phases in which the crack propagates should also be considered along with the crack path deviation. Higher fatigue crack growth rates in ferritic regions were also observed in a previous paper on the fatigue behavior of sinter-hardened PM steels [27] as well as reported by Deng et al. [20]. Therefore, care should be taken when selecting PM steels for applications where fatigue resistance is important. Chemistry as well as alloying strategy should be selected to minimize the formation of Ni-rich ferrite.

5. Conclusions

In the present study, the effect of microstructure heterogeneity on fatigue crack propagation was studied to better understand the fatigue crack growth behavior of two common PM steels with heterogeneous and homogeneous microstructures. The main findings of our work are summarized as follows:

Fatigue crack growth rates in both types of alloys increased by increasing the *R*-ratio. This was the result of the higher monotonic contribution and strain localization at the crack tip by increasing minimum loads. PM steel with a homogenous microstructure showed slightly higher sensitivity to the strain localization and crack tip plasticity.

Different crack closure mechanisms were involved in both PM steels, which have caused the observed anomaly in the variation trend of crack closure versus the *R*-ratio. Plasticity induced crack closure caused by the plastically deformed area in the wake of the crack as well as the roughness-induced crack closure caused by the crack deflection and/or the mixed mode sliding of the crack faces acting synergistically are the most probable mechanisms.

Profile roughness parameter (R_L) was larger than 1 for both PM steels at all tested *R*-ratios showing the tortuous and deflected crack path in both heterogeneous and homogeneous microstructures. The presence of a considerable amount of pearlite in both alloys was found to be the reason for the observed deflection, since cracks had their path significantly deviated when facing the hard cementite lamellae. The crack path was longer and more deviated in the heterogeneous microstructure of the admixed PM steel because of the Ni-rich ferritic rings around the pearlitic grains. The fatigue fracture surfaces showed that the prinicpal mode of fracture was the intergranular one, but by increasing the *R*-ratio the percentage of transgranular, fracture increased.

Although the presence of Ni-rich ferritic rings around the pearlitic grains in heterogeneous microstructure PM steel have caused the more deviated crack path, the fatigue crack growth rates in this alloy were almost identical to the pre-alloyed one with homogeneous microstructure, which indicates that the crack propagates faster in Ni-rich ferrite than in pearlite. This higher propagation rate is counterbalanced by the crack deviation and led to the same FCGs in both microstructures. The crack passed along the prior particle boundaries where the retained austenite was located, but it did not pass through this phase, indicating that austenitic regions do not constitute preferable paths compared to Ni-rich ferritic areas. The statistical analysis of the other half of the fracture surface verified the conclusions made on the effect of each phase on the crack propagation.

PM steels to be used in applications where fatigue resistance is a dominant factor should be engineered to minimize the formation of Ni-rich ferritic areas.

Acknowledgments: The authors would like to acknowledge the Natural Science and Engineering Research Council of Canada (NSERC (Grant No.: 210856817)) as well as the Network of Centers of Excellence—Auto21 (Grant No.: C502-CPM) for their financial support.

Author Contributions: Mousavinasab and Blais conceived and designed the experiments; Mousavinasab performed the experiments; Both authors analyzed the data; Mousavinasab wrote the paper and Blais reviewed it before submission.

Conflicts of Interest: The authors declare no conflict of interest.

References

1. Cimino, T.M.; Rutz, H.G.; Graham, A.H.; Murphy, T.F. The Effect of Microstructure on Fatigue Properties of Ferrous P/M Materials. *Adv. Powder Metall. Part. Mater.* **1997**, *2*, 13.
2. Rutz, H.; Murphy, T.; Cimino, T. The effect of microstructure on fatigue properties of high density ferrous P/M materials. *Adv. Powder Metall. Part. Mater.* **1996**, *4*, 13.
3. Abdoos, H.; Khorsand, H.; Shahani, A.R. Fatigue behavior of diffusion bonded powder metallurgy steel with heterogeneous microstructure. *Mater. Des.* **2009**, *30*, 1026–1031. [CrossRef]
4. Danninger, H.; Spoljaric, D.; Weiss, B. Microstructural features limiting the performance of P/M steels. *Int. J. Powder Metall.* **1997**, *33*, 43–53.
5. Holmes, J.; Queeney, R.A. Fatigue crack initiation in a porous steel. *Powder Metall.* **1985**, *28*, 231–235. [CrossRef]
6. Gerard, D.A.; Koss, D.A. Low cycle fatigue crack initiation: modeling the effect of porosity. *Int. J. Powder Metall.* **1990**, *26*, 337–343.
7. Polasik, S.; Williams, J.J.; Chawla, N.; Narasimhan, K.S. Fatigue crack initiation and propagation in ferrous powder metallurgy alloys. *Adv. Powder Metall. Part. Mater.* **2001**, 10–172.
8. Carabajar, S.; Verdu, C.; Hamel, A.; Fougeres, R. Fatigue behaviour of a nickel alloyed sintered steel. *Mater. Sci. Eng. A* **1998**, *257*, 225–234. [CrossRef]
9. Saritas, S.; Causton, R.; James, B.; Lawley, A. Effect of Microstructural Inhomogeneities on the Fatigue Crack Growth Response of a Prealloyed and Two Hybrid P/M Steels. *Adv. Powder Metall. Part. Mater.* **2002**, *5*, 5–136.
10. Murphy, T.F.; Lindsley, B.A.; Schade, C.T. A metallographic examination into fatigue-crack initiation and growth in ferrous PM materials. *Int. J. Powder Metall.* **2013**, *49*, 23–34.
11. Polasik, S.J.; Williams, J.J.; Chawla, N. Fatigue crack initiation and propagation of binder-treated powder metallurgy steels. *Metall. Mater. Trans. A* **2002**, *33*, 73–81. [CrossRef]
12. Andersson, O.; Lindqvist, B. Benefits of heterogeneous structures for the fatigue behaviour of PM steels. *Met. Powder Rep.* **1990**, *45*, 765–768. [CrossRef]
13. Bergmark, A.; Alzati, L. Fatigue crack path in Cu-Ni-Mo alloyed PM steel. *Fatigue Fract. Eng. Mater. Struct.* **2005**, *28*, 229–235. [CrossRef]
14. ASTM International. *Standard Test Method for Measurement of Fatigue Crack Growth Rates*; ASTM International: West Conshohocken, PA, USA, 2011.
15. Nabeel, M. Diffusion of Elemental Additives during Sintering. Master's Thesis, Royal Institute of Technology, Stockholm, Sweden, 2012.
16. Wu, M.; Hwang, K. Formation mechanism of weak ferrite areas in Ni-containing powder metal steels and methods of strengthening them. *Mater. Sci. Eng. A* **2010**, *527*, 5421–5429. [CrossRef]
17. Tougas, B.; Blais, C.; Larouche, M.; Chagnon, F.; Powders, R.T.M.; Pelletier, S. Characterization of the Formation of Nickel Rich Areas in PM Nickel Steels and Their Effect on Mechanical Properties. *Adv. Powder Metall. Part. Mater.* **2012**, *5*, 19–33.
18. Meyers, M.A.; Chawla, K.K. *Mechanical Behavior of Materials*; Cambridge University Press: Cambridge, UK, 2009; Volume 547.
19. Krupp, U. *Fatigue Crack Propagation in Metals and Alloys*; Wiley: New York, NY, USA, 2007.
20. Deng, X.; Piotrowski, G.; Chawla, N.; Narasimhan, K. Fatigue crack growth behavior of hybrid and prealloyed sintered steels: Part II. Fatigue behavior. *Mater. Sci. Eng. A* **2008**, *491*, 28–38. [CrossRef]

21. Sadananda, K.; Vasudevan, A.K. Crack tip driving forces and crack growth representation under fatigue. *Int. J. Fatigue* **2004**, *26*, 39–47. [CrossRef]
22. Sadananda, K.; Vasudevan, A.K. Fatigue crack growth mechanisms in steels. *Int. J. Fatigue* **2003**, *25*, 899–914. [CrossRef]
23. Elber, W. The significance of fatigue crack closure. In *Damage Tolerance in Aircraft Structures*; ASTM International: West Conshohocken, PA, USA, 1971.
24. Schijve, J. *Fatigue of Structures and Materials*; Springer: New York, NY, USA, 2001.
25. Schijve, J. Fatigue of structures and materials in the 20th century and the state of the art. *Int. J. Fatigue* **2003**, *25*, 679–702. [CrossRef]
26. Bathias, C. *Fatigue of Materials and Structures*; Wiley: New York, NY, USA, 2013; Volume 53.
27. Mousavinasab, S.; Blais, C. Study of the effect of microstructure heterogeneity on fatigue crack propagation of low-alloyed PM steels. *Mater. Sci. Eng. A* **2016**, *667*, 444–453. [CrossRef]
28. Murphy, T.F. Evaluation of PM fracture surfaces using quantitative fractography. *Int. J. Powder Metall.* **2009**, *45*, 49–61.
29. Gokhale, A.; Underwood, E. A general method for estimation of fracture surface roughness: Part I. Theoretical aspects. *Metall. Trans. A* **1990**, *21*, 1193–1199. [CrossRef]
30. Piotrowski, G.B.; Deng, X.; Chawla, N.; Narasimhan, K.S.; Marucci, M.L. Fatigue-Crack Growth of Fe-0.85Mo-2Ni-0.6C Steels with a Heterogeneous Microstructure. *Int. J. Powder Metall.* **2005**, *41*, 31–41.